1986-8

~~1987-7~~

Geochemistry of Slave Province Volcanic Rocks: Yellowknife Belt

by

A.M. Goodwin

Northern Affairs
APR 23 1986
Yellowknife, N.W.T.
Geology Division

December, 1985

Department of Geology
University of Toronto
Toronto, Canada M5S 1A1

"corrected, preliminary copy"

88-02994/

ABSTRACT

Systematic sampling and analysis of Yellowknife volcanic rocks have provided mean class compositions and mean compositions by segment, cycle, and formation. The Yellowknife assemblage constitutes a modified bimodal volcanic succession. Ni-Sr plots indicate that Lower Kam lavas are products of mainly fractional crystallization processes, and Upper Kam lavas of mainly partial fusion processes, the respective mantle sources contrasting in Ni-Sr abundances. The bulk of the volcanic components, dominated by basalt and basaltic-andesite, could be products of differentiation processes involving more or less common mantle sources. However, the separate and distinct character of the felsic volcanic components without significant intervening intermediate components suggests a separate origin such as the melting of sialic crust. Further chemical data are required to investigate this posibility.

In general, the Yellowknife volcanic association has trace element characteristics (F1 group) that are considered to be unfavourable for the presence of massive base metal sulfide deposits. However other Slave Province associations include the favourable F3 group of felsic metavolcanic horizons.

ACKNOWLEDGMENTS

I am grateful to W.A. Padgham for full support in the Yellowknife field are. and to Carol Ellis for her able assistance in the sampling program. S. Shanbhag, University of Toronto. prepared the illustrations.

Geochemistry of Slave Province Volcanic Rocks· Yellowknife Belt

Introduction

The Yellowknife Greenstone Belt lies at the western margin of the Yellowknife Supracrustal Basin (Henderson, 1981) a dominantly turbidite-filled Archean depository with subordinate, mainly peripheral, volcanic-rich greenstone belts. The Basin extends 120 km to the east of Yellowknife and 170 km to the north from its southern limit where terminated at a late fault along Hearne Channel of Great Slave Lake. Other greenstone belts bordering this greywacke-mudstone-filled basin include: Clan Lake belt, 50 km north of Yellowknife; Thistlewaite belt, 40 km still further northeast; and Cameron River and Beaulieu River belts respectively 80 and 120 km northeast of Yellowknife, both located at or near the eastern margin of the basin. The turbidites, which underlie approximately 90 percent of the Yellowknife Supracrustal Basin, constitute the type sediments of the Yellowknife Supergroup (Henderson, 1970). In all, Slave Province includes at least five such Archean supracrustal basins of which Yellowknife Basin is the southernmost and High Lake Basin, 700 km to the north, the northernmost.

Numerous granitoid plutons have intruded metasupracrustal rocks of the Yellowknife Basin, commonly folding and contorting them. Metamorphic grade in the basin is typically greenschist to amphibolite facies, rising to upper amphibolite facies near intrusive contacts.

Older granitoid rocks, commonly tonalitic to trondhjemitic gneiss, migmatite, and minor granite and granodiorite, locally with felsic volcanic and metasedimentary enclaves, have been identified in Slave Province, for example, at the northern and southern extremities of the Yellowknife greenstone belt. Structural development of the Yellowknife Supracrustal Basin has been attributed to rifting of this pre-metasupracrustal sialic basement (Henderson, 1981).

Available geochronologic data indicate that Yellowknife sedimentation and volcanism occurred in an abbreviated 20-Ma interval, from 2680 to 2660 Ma ago, upon or near 2700 to 3200 Ma-old sialic crust; this was quickly followed by regional syntectonic plutonism and metamorphism at 2660 to 2620 Ma. Thus complete Yellowknife belt development occurred in an interval not exceeding 60 Ma (Easton, 1984; Lambert et al., 1984).

Two main types of Archean volcanic successions have been recognized in Slave Province: 1) Yellowknife-type, grossly similar to Superior Province belts, with thick basalt-rich lower phases capped by subordinate intermediate-to-felsic units, and 2) basalt-poor Hackett River-type, dominated by felsic volcanic rocks (Padgham, unpublished). Interestingly, komatiite or other ultramafic volcanic rocks have not been reported so far in Slave Province.

Slave Province has produced more than 12 million ounces of gold, 88 percent derived from mines in gold-silver-bearing quartz-carbonate-sericite shear zones cutting Yellowknife volcanic rocks. The recently activated Lupin Mine will produce a major part of the provinces's gold production from amphibolitic silicate-sulfide banded iron formation interstratified with metaturbidites of the Point Lake-Contwoyto Lake Supracrustal Basin located in the centre of Slave Province. Volcanogenic base metal sulfide deposits have been found in nine volcanic belts of Slave Province. Of these, the High Lake deposit, located in High Lake Supracrustal Basin, centred 600 km north of Yellowknife and 100 km south of Coronation Gulf, contains established reserves of 5.2 million tons grading 3.5% Cu, 2.5% Zn, 0.6 ozs/T Ag, 0.2 ozs/T Au, and minor Pb. In addition, numerous Li-Be-Sn-W-Ta-bearing pegmatites are present in the Province (Padgham, unpublished report).

The purpose of this study is to chemically characterize the Yellowknife volcanic succession by volcanic class, stratigraphic segment, and belt as a basis for eventual geochemical comparison with other Slave Province greenstone belts and other greenstone terrains.

Yellowknife Volcanic Belt

The north-trending volcanic belt at Yellowknife is 5 km wide and 52 km long. The volcanic rocks form a broad homocline of northeast trending, near-vertical, southeast facing units cut by numerous northerly trending, mainly sinistral sub-vertical faults. Of the latter, Kam, West Bay and Akaitcho faults have effected major stratigraphic offsets up to 5000 m. The resulting structural segments, taken together, form a continuous stratigraphic section estimated at 14,000 m (Baragar, 1966).

The lower contact of the Yellowknife volcanic section to the west is about equally shared by faulted and intrusive contacts, the latter against younger granitoids. Only at the northern and southern extremities of the belt is the apparent base of the section preserved and exposed. Thus to the north a substantial area of granitoid gneiss contains felsic metavolcanic enclaves; and to the south a 750 m-thick unit of mafic flows, clastics and felsic volcanic rocks (Octopus Formation) is interpreted as the product of an older volcanic-sedimentary cycle unconformably underlying the Kam Formation (Helmstaedt et al., 1979).

The Kam Formation is composed mainly of mafic lava flows including massive (43%), pillowed (42%) and variolitic (11%) phases. Felsic tuffs and flows (4%) form a prominent zone (Townsite or Brock Flows) composed of coarsely fragmental to densely porphyritic rocks containing at least one pillowed lava flow, located at about mid-thickness of the Kam succession. Similar felsic pyroclastic rocks (Banting Formation) unconformably overlie upper Kam mafic volcanic rocks and form the uppermost volcanic division in the belt. On this basis Baragar (1966) allowed for two volcanic cycles, the lower cycle (Lower Kam) terminated by the Townsite Flows: at mid-thickness; and the upper cycle comprising the Upper Kam lavas (Upper Kam) plus the overlying Banting Formation. Recent work has raised considerable uncertainty as to the true stratigraphic relations of Upper Kam, Banting, and the intervening dominantly metasedimentary Walsh and Jackson Lake Formations. However, for present

purposes, a straight-forward stratigraphic arrangment will suffice, comprising (Table 1): Lower Kam = segments A + B + Townsite Flows; Upper Kam = segments C, D, E; and Banting Formation = segment F.

As discussed below, Lower Kam, including Townsite Flows, constitutes the first main mafic-to-felsic volcanic cycle; Upper Kam segments C, D and E^1 constitute the second main cycle; and Upper Kam segment E^2 constitutes a third, subordinate, mafic-to-felsic volcanic cycle. These three volcanic cycles are unconformably overlain by Banting felsic pyroclastic rocks (segment F) with or without intervening metasediments.

Sampling Procedure

During the 1983 field season, 47 stratigraphically controlled volcanic units were sampled including 42 Kam and 5 Banting samples. All are chip samples composed either of fresh volcanic fragments taken at regular intervals across selected outcrops (35 samples) or of diamond drill intersections (12 samples). In general, samples were spaced at approximately regular intervals of 350 m across the Kam and Banting Formations.

The pattern of sampling closely follows Baragar's (1966) stratigraphic scheme (segments A-F) with the following exceptions: segment B was samples in 1983 west of, rather than east of, Akaaitcho and West Bay Faults; segment F (Banting Formation) was sampled in 1983 exclusively in diamond drill intersections (DDH 1158 and 1157); only the upper part of segment A was sampled in 1983; and finally, Segment D was sampled twice in 1983, once in outcrop (7 samples) and once in drill intersections, DDH 919 and 1159 (7 samples).

The stratigraphic scheme including formations, segments, cycles and samples are summarized in Table 1.

All samples were crushed and ground for chemical analysis by XRF (Cr, Ni, V, Sr, Zr, Y, Sr, Rb) and INAA (REE, Th, Hf, Ta, Ba, Sc, Co) techniques at the University of Toronto. Major elements were determined by XRF at University of Durham, England, by

by J.G. Holland. All major element analyses (weight percent) have been recalculated to 100% volatile- and P_2O_5-free. All trace elements are reported in ppm.

Stratigraphy

The stratigraphic scheme (formations, segments, cycles) and corresponding sampling are summarized in Table 1. Thus the Kam Formation divides naturally into Lower Kam, 6500 m thick, comprising segments A + B + Townsite Flows; and Upper Kam, 6800 m thick, with segments C, D and E. Banting Formation, 700 m thick, comprises segment F. The volcanic succession also divides naturally into two main mafic-to-felsic cycles and one subsidiary cycle, eacy cycle marked by comparatively thick uniform basalt flows capped by thin felsic-intermediate volcanic units. The present cyclic divisions essentially follow those of Baragar (1966), two points of difference being: 1) Cycle 2 is terminated with segment E^1 rather than with F (Banting), and 2) E^2, previously demarcated chemically though not tabulated independently by Barager (1966, Fig. 4), is elevated to the status of subsidiary cycle 3. The present scheme thereby divorces Banting felsic volcanic rocks from the Kam succession in recognition of their possible genetic independence (see below).

Classification

A simple SiO_2-based classification is used: basalt -- <53%; basaltic andesite -- 53-57%; andesite -- 57-63%; dacite -- 63-70%; and rhyolite -- >70%. As sampled in 1983, rhyolite is absent in the Yellowknife belt, the highest SiO_2 content recorded being 68.3% (Townsite Flows). This corresponds closely with Baragar's 1966 results.

According to the 1983 sampling, the Yellowknife volcanic succession is composed of the following class percentages, with the number of samples in brackets (Table 2): basalt -- 62% (29); basaltic andesite -- 17% (8); andesite -- 8% (4); and dacite -- 13% (6). Baragar's previous estimate (Baragar and Goodwin, 1969), based on greater sampling density (approximately 80 samples) and a normative-based classification, is: basalt -- 60%; classes "A + B" -- 7%; andesite -- 18% and salic -- 14%. Assuming that the present classes of basaltic andesite + andesite (= 25%) are equivalent to

Baragar's classes "A + B" + andesite (= 25%). then the two results are in close agreement.

Analytical Results

The main chemical results are tabulated in Tables 3, 4 5. Similar results from other greenstone belts in Slave Province are expected to lead to meaningful Province-wide inter-belt geochemical comparisons.

Mean Class (Table 3)

The mean class compositions with standard deviations provide the fundamental chemical framework of the Yellowknife belt. Major element compositions by class compare closely, for the most part, with those previously calculated by Baragar (Baragar and Goodwin, 1969). The notable exception lies in andesite which, according to the 1983 sampling, has significantly higher SiO_2 (62.5 vs 56.7%) and K_2O (1.67 vs. 0.59%); these contrasts are due mainly, though not completely. to different classification systems. Insofar as available for comparison, mean trace element compositions based on the 1983 sampling show similar levels of abundances to Baragar's previous calculations in basalt, but substantially higher levels of Ba, Zr and Co in andesite and dacite.

Trace element trends across the 4 classes correspond, for the most part, to those in a standard mafic-to-felsic igneous progression. Thus the mean abundance levels of incompatible elements (e.g. Ba, Sr, Rb, Th) increase; of transition elements (e.g. Ni, Cr, V, Co) decrease; of REE and LREE increase; and of HREE decrease. Basalt-andesite stands in anomalous exception to these trends with respect to both transition elements and REE. It is not known at present whether this is a true expression of this particular class composition, or is simple due to unrepresentative sampling.

Stratigraphic Divisions (Table 4)

Mean compositions by stratigraphic division (Table 4) provide insight into the composition of the volcanic rocks by segment. cycle. division. formation and belt.

Segments A, B, C, and D + E[1] (cols. 1,2,5 and 6 respectively), which represent the bulk of the Yellowknife mafic volcanic rocks, reveal the following trends: consistently declining FeO, TiO_2 and MnO levels; consistently increasing MgO levels; and inconsistent levels in transition elements and REE. Cycle 3 (col. 8), with high FeO, TiO_2 and MnO levels, very high REE and incompatible element levels, yet unusually low transition element levels, stands apart from these general trends.

Mean Class Composition by Division (Table 5)

Mean class compositions by segment, cycle and formation (Table 5) provide direct comparisons by class across (i.e. from base to top) the stratigraphic column. Similar chemical trends are revealed to those in Table 4. Thus the bulk of the basalts, arranged in sequence (cols. 1,2,5,6), reveal 1) decreasing FeO, TiO_2 and MnO levels, yet 2) increasing MgO level; 3) decreasing REE, LREE and HREE levels, yet 4) generally increasing $[La/Yb]_N$ and $[/sn/Yb]_N$ levels. and 5) inconsistent incompatible and transition element levels.

SiO_2 Histogram (Fig. 2)

A SiO_2 histogram of a) Kam + Banting Formations, b) Lower Kam, and c) Upper Kam (Fig. 2 a,b,c) illustrates the essential bimodal character of the Yellowknife Belt volcanic succession. Lower Kam (Fig. 2b), (N.B. including Townsite Flows) with mean SiO_2 = 53.66%, comprises basalt (55%), basaltic-andesite (27%) and some high-SiO_2 dacite (18%), the latter exclusively Townsite Flows. The the Lower Kam sequence lacks intermediate SiO_2 values (57-67%). Upper Kam (Fig. 2c), (N.B. excluding Banting felsic units) with mean SiO_2 = 50.67%, comprises basalt (74%), basaltic-andesite (16%), and andesite (10%). The Upper Kam SiO_2 gap is only 4% (57-161). Kam + Banting combined (Fig. 2a), with mean SiO_2 = 53.02% comprise basalt (62%), basaltic andesite (17%), andesite (8%), and dacite (13%). Thus the volcanic succession is composed of repeated alternations of thick low-SiO_2 and thin high-SiO_2 units. There is no obvious quantitative relationship between the respective low-SiO_2 and high-SiO_2 parts. Intermediate SiO^2 values (53-63%). though rare. are present in

the Yellowknife assemblage which is, therefore, more appropriately classified as a modified bimodal volcanic succession.

AFM Diagram (Fig. 3)

Of nine Lower Kam samples (segments A, B in Table 4), eight (nos. 1-8 in Table 1) plot in, or on the oundary of, the tholeiite (TH) field of the AFM diagram (Fig. 3a); and one (no. 9) falls in the calc-alkaline (CA) field, but close to the TH boundary. the remaining two Lower Kam samples (nos. 10, 11), both of Townsite Flows units, plot well within the CA field.

Thirty-one Upper Kam samples (segments C, D, E and E^2 in Table 4; sample nos. 12-42 in Table 1) plot almost equally in the TH (16 samples) and CA (15 samples) fields (Fig. 3b). The CA components comprise eleven samples (nos. 12, 17-22, 25, 27, 28, 42 of segments C and D) lying close to the TH boundary, and four samples (Nos. 29-31, 35 of segments E^1 and E^2) at a greater distance from the F-M tie-line. Finally, the five Banting samples (nos. 43-47 of segment F) occupy the same isolated part of the CA field as do the Townsite Flow samples in Figure 3a.

Comparison with Table 1 reveals that the majority (14 of 18) of Kam CA samples occupy upper stratigraphic positions in their respective segments i.e. segments B (no. 9), C (nos. 17-21), D^1(nos. 25, 27, 28), D^2(no. 42), E^1 (nos. 29-31), and E^2 (no. 35). Thus each segment (i.e. B-E) represents a chemical compositional gradation with a lower thicker TH zone and an upper thinner CA zone. Furthermore the presence of preponderant (15 of 18) of CA units in the Upper Kam division demonstrates an overall TH-CA chemical progression. Most CA units lie close to the TH boundary in proximity to and in possible genetic relationship with the TH units. In sharp contrast Townsite and Banting felsic units (Figs. 3a, b) respectively occupy identical, isolated positions thereby allowing of a common origin distinct from associated mafic units.

Ni-Sr (Fig. 4)

A log-log plot of Ni-Sr provides insight into the relationship of incompatible (Sr) and compatible (Ni) elements. Compatible element abundances are controlled mainly by processes of crystallization differentiation whereas those of incompatible elements are influenced mainly by partial fusion. The plot thereby reveals the relative influences of these two main magma-forming processes.

Fig. 4a shows Ni-Sr plots for the eleven Lower Kam samples, the upper nine plots being those of segments A,B and the two lower plots those of Townsite Flows. The predominant vertical trends, parallel to the compatible element (NI) axis, are apparent. The upper sub-vertical line to the left represents segment A; the companion sub-vertical line to the right represents segment B, with sample no. 9 which is located at the stratigraphic top of segment B, dramatically offset to the right on a line approximately parallel to the incompatible element (Sr) axis. The two Townsite Flow samples plot on a vertical line in the lower part of the diagram, significantly offset along the Ni axis with respect to the rest of the Lower Kam samples.

Fig. 4b is the comparable Ni-Sr plot for the thirty-six Upper Kam and Banting samples. All but one (no. 35 from the top of segment E^2) of the 31 Upper Kam samples plot in a generally subhorizontal oval zone lying between 40-150 ppm Ni and 30-200 ppm Sr that is sub-parallel to the horizontal incompatible element (Sr) axis. Sample no. 35 plots vertically below this zone (33 ppm Ni-80 ppm Sr) and close to the trend described by Lower Kam samples (Fig. 4a). The five Banting samples describe a generally vertical trend somewhat offset to the lower right of the main Upper Kam zone, yet with significantly higher Ni-Sr abundances than the two corresponding felsic Townsite Flows (Fig. 4a).

The genetic implications of these trends are discussed below. In the meantime, in terms of regional structure, the sharp compositional contrast between Lower Kam and Upper Kam rocks renders unlikely any attempt to stratigraphically correlate them. thus the data do not support the proposed stratigraphic correlation on

structural grounds (Helmstaedt et al.. 1979) of Kam Point sill (plus felsic fragmental rocks) with Townsite Flows (plus sill) which would result in Lower Kam and Upper Kam volcanic rocks being one and the same sequence.

$[La/Yb]^n$ - $[Yb]_n$ (fig. 5)

This diagram provides a view of light REE represented by La, and heavy REE (represented by Yb) abundances and corresponding enrichment-depletion trends in the volcanic rocks. In general, a vertical trend parallel to the $[La/Yb]_N$ axis is in the direction of enriched La and depleted Yb contents, whereas a horizontal trend represents changes in Yb content alone. Areas I-V represent arbitrary divisions of the general field of Archean volcanic rocks (Goodwin, unpublished). Most tholeiitic basalt-komatiite lavas plot in or close to area III. The common mafic-felsic volcanic trend is in a sub-vertical direction from Area III across Area II to Area I. A less common trend, but one of metallogenic significance, is sub-horizontallyinclined to the upper right from Area III to Areas IV and/or V.

Cycle I mafic volcanic samples (I) plot in Area III and the adjoining part of Area II. The two Townsite Flows felsic samples (T) plot vertically above in area I ($[La/Yb]_N$ 10), Cycle 2 mafic volcanic samples (IIa) plot in a field that incorporates most of that of Cycle 1 mafic lavas, but in addition, extends significantly both below, i.e. lower La/Yb, and above, i.e. higher La/Yb. The more evolved Cycle 2 andesite flows of segment E^1 (IIb) plot on the Area I-II boundary close to but slightly offset from the Townsite Flows (T). Cycle 3 volcanic samples (III), comprising three basalts and one basaltic-andesite, plot mainly in Area II in a subvertical field extending from fields I and IIa in the lower right to field IIB and slightly beyond in the upper left. Finally, Banting felsic volcanic samples (B) plot high in Area I, in the extreme upper La/Yb position for the Yellowknife assemblage.

Cycles I and II thereby present similar patterns: 1) stratigraphically lower mafic components have conventionally low $[La/Yb]_N$ = 1.5-2 and 2) upper components

Cycles I and II thereby present similar patterns: 1) stratigraphically lower mafic components have conventionally low $[La/Yb]_N$ = 1.5-2. and 2) upper components have elevated $[La/Yb]_N$ = 8-11. Cycle III field is basically similar with, however, the mafic components occupying a comparatively high La/Yb position.

In summary, Cycle I and Cycle II mafic volcanic rocks cover similar fields except for the upper prolongation of Cycle II. Cycle III field has significantly higher La/Yb, in this regard resembling the upper prolongation of Cycle II. The intermediate-felsic components of the three cycles occupy similar fields at or near the Area I-II boundary. Banting components are the most highly evolved Yellowknife volcanic rocks. The fundamental Yellowknife cyclic pattern is expressed, then, in the rythmic alternation of lower and higher La/Yb stratigraphic parts.

Discussion

Petrogenesis

The essential bimodal character of the Yellowknife volcanic succession (Fig. 2) with, however, significant basaltic-andesite and some andesite components, can be interpreted as 1) products of processes of magma differentiation from a mantle source(s) (crystallization differentiation or partial fusion), 2) involvement of two distinct magma sources, namely mantle and pre-existing continental crust, or 3) some combination of these two. The present data do not provide an unequivocal answer to this fundamental problem of magma genesis. On the one hand, the cyclic development the bulk of the volcanic components, dominated by basalt and basaltic-andesite components with their conventional TH-CA progressions, could be products of differentiation processes involving more or less common mantle sources. However, the separate and distinct character of the felsic volcanic components, without significant intervening intermediate components, suggests a completely separate origin for the felsic volcanic rocks such as the melting of sialic crust. Additional data, especially isotopic ratios (Sr-Rb and Sm-Nd) would be required to resolve this.

Whatever the source of the felsic components, it seems clear that the Lower Kam and Upper Kam mafic components are products of different processes of differentiation and probably involving different mantle sources (Fig. 4). Lower Kam lavas are indicated to be products of fractional crystallization processes of mantle-derived material containing >300 ppm Ni and 90-150 ppm Sr. Upper Kam lavas, on the other hand, were apparently derived by partial fusion processes from a mantle source with 100-150 ppm Ni and <30 ppm Sr. Thus there appears to be a fundamental change in both source and process at the Lower-Upper Kam boundary.

A possible solution is provided by a mantle diapir mechanism whereby the earlier mantle source of Lower Kam (Cycle I) would be overwhelmed by the rising, compositionally changing mantle source of, successively, Cycles II and III. The simplest method of introducing the felsic volcanic components is to allow for periodic fusion of older sialic crust. However, as stated above, other geochemical data are required to test the feasibility of this hypothesis.

Metallogenesis

Felsic metavolcanic horizons studies in 13 varied Archean volcanic piles in Superior SProvince have been divided into 3 major groups based on trace element geochemistry (Lesher et al., in press) and following the system of Condie (1976), with the following metallogenic aspects:

1. F1 group: dacite and rhyolite. Steep REE patterns $[La/yb]_N$ = 6-34; weakly negative to moderately positive Eu anomalies; high Sr and Zr/Y (9-31); low abundances of high field strength (HFS) elements (Th, U, Zr, Hf). Representative horizons have been identified in 7 volcanic piles. None of the F1 group horizons, as known, host base metal sulfide horizons.

2. F2 group: rhyodacite and rhyolite. Gently sloping REE patterns $[La/Yb]_N$ = 2-6; variable Eu anomalies; moderate Zr/Y (6-11); and intermediate abundances of HFS elements and Sr. Representative horizons have been identified in 4 volcanic piles.

Only F2 group horizons in the Sturgeon Lake volcanic pile host base metal sulfide deposits.

3. F3 group: rhyolite and high- SiO_2 rhyolite. Relatively flat REE patterns $[La/Yb]_n$ = 1-4; with either a) variable but generally moderately negative Eu anomalies, low Zr/Y (4-7), high Sc, and intermediate HFS element abundances; or b) pronounced negative Eu anomalies. Located so far in 6 volcanic piles. All of the F3 group horizons, with one exception (Garrison in Ontario) host important base metal sulfide deposits.

These results demonstrate the variety of felsic volcanic rocks present in the greenstone belts, and some metallogenic implications. The geochemical variations are attributed mainly to petrogenetic differences involving local felsic differentiation in high level magma chambers which also may have influenced the formation of massive base metal sulfide deposits (Campbell et al., 1985).

Figure 5 and Tables 3-5 reveal clearly that Yellowknife volcanic rocks correspond to F1 group, namely those associations in which the felsic components have steep REE patterns, insignificant Eu anomalies, high Sr and Zr/Y, and comparatively low abundances of high field strength elements. According to the model, this association is unfavourable for the presence of massive base metal sulfide deposits.

Figure 5 further shows the field of all available REE analyses from Slave Province including 55 samples from the Cameron River and Beaulieu River greenstone belts and 6 samples from the High Lake belt (unpublished data). The composite Slave Province $[La/Yb]_n$ - $[Yb]_n$ field has a significant extension subparallel to the high $[Yb]_n$ axis, which is in the direction of the favourable F3 group of felsic metavolcanic horizons. A study of the metallogenic significance and implications of the Cameron River Beaulieu River data is presently underway.

Illustrations

Figures

Fig. 1 Generalized geology and sample locations, Yellowknife Greenstone Belt.

2 SiO_2 histogram of 47 Yellowknife samples

3 AFM plot of a) Lower Kam and b) Upper Kam and Banting samples

4 Ni-Sr long-log plot a) Lower Kam and b) Upper Kam

5 $[La/Yb]_n$ - $[Yb]_n$ plot of Yellowknife volcanic rocks in relation to Slave Province field

Tables

Table 1 Stratigraphic divisions, thicknesses, and sampling of Yellowknife Greenstone Belt.

2 Number of samples by class and stratigraphic division in the Yellowknife Greenstone Belt.

3 Mean class composition, Yellowknife Belt.

4 Mean compositions by stratigraphic divisions, Yellowknife Belt.

5 Mean class compositions by segment, cycle, and formation in the Yellownife Belt.

Baragar, W.R.A., 1966. Geochemistry of the Yellowknife volcanic rocks. Can. Jour. Earth Sci., v. 3, p. 9-30.

Baragar, W.R.A. and Goodwin, A.M., 1966. Andesites and Archean volcanism of the Canadian Shield. In Proceedings of the Andesite Conference; edited by A.R. McBirney; Oregon Department of Geology and Mineral Industries, Bulletin 65, p. 121-142.

Baragar, W.R.A., 1975. Miscellaneous data from volcanic belts at Yellowknife, Wolverine Lake, and James River, N.W.T. Geol. Surv. Canada, Paper 75-1, part A, p. 281-286.

Campbell, I.H., McDougal, T.J. and Turner, J.S., 1985. A note on the fluid dynamic processes which can influence the deposition of massive sulfides. Economic Geology, v. 79, p. 1905-1913.

Capdevila, R., Goodwin, A.M., Ujike, O. and Gorton, M.P., 1982. Trace-element geochemistry of Archean volcanic rocks and crustal growth in southwestern Abitibi belt, Canada. Geology, v. 10, p. 418-422.

Condie, K.C., 1976. Trace-element geochemistry of Archean greenstone belts. Earth-Science Reviews, 12, p. 393-417.

Easton, R.M., 1984. Compilation of geochronologic data for the Yellowknife greenstone belt (85J/8, 85J/() and vicinity, District of Mackenzie, N.W.T. In Contributions to the Geology of the Northwest Territories; edited by J.A. Brophy; D.I.A.N.D., EGS 1984-6, p. 1-20.

Goodwin, A.M., 1977. Archean volcanism in Superior Province, Canadian Shield. In: W.R.A. Baragar, L.C. Coleman and J.M. Hall (editors), Volcanic Regimes in Canada. Geol. Assoc. Canada, Special Paper 16, p. 205-241.

Goodwin, A.M., 1984. Some geochemical patterns in Yellowknife Supergroup metavolcanic rocks, Yellowknife area, Slave Province. Unpublished report.

Helmstaedt, H., King, J., Goodwin, J.A. and Patterson, J.G., 1979. Geology of the southwest end of the Yellowknife greenstone belt. In Procedings of the Gold

Henderson, J.F. and Brown, I.C., 1966. Geology and structure of the Yellowknife greenstone belt, District of Mackenzie. Geol. Surv. Canada, Bulletin 141.

Henderson, J.B., 1970. Stratigraphy of the Archean Yellowknife supergroup; Yellowknife Bay - Prosperous Lake area, District of Mackenzie. Geol. Surv. Canada, Paper 70-26.

Lambert, R. St. J., Chamberlain, V.E. and Cunningham, M., 1984. Sm-Nd age and petrogenesis of Yellowknife Group volcanics, N.W.T. Geol. Assoc. Canada, program with Abstracts, v. 9, p. 81.

Lesher, C.M., Goodwin, A.M., Campbell, I.H. and Gorton, M.P., in press. Trace-element geochemistry of ore-associated and barren felsic metavolcanic rocks in Superior Province, Canada. Can. Jour. Earth Sci.

Padgham, W.A., 1979. Geology of the Yellowknife volcanic belt. Proceedings of the Gold Workshop. Yellowknife; p. 288-322.

Padgham, W.A., 1979. Gold deposits of the Northwest Territories. Proceedings of the Gold Workshop, Yellowknife, p. 174-200.

Padgham, W.A., 1980. An Archean ignimbrite at Yellowknife and its relationship to the Kam Formation basalts. Precambrian Research, v. 12, p. 99-113.

Padgham, W.A., 19 Observations and speculations on supracrustal successions in the Slave Structural Province. In Evolution of Archean Supracrustal Sequences, edited by L.D. Ayres, P.C. Thurston, K.D. Card and W. Weber; Geol. Assoc. Canada, special Paper 28, p. 133-152.

Padgham, W.A., 1984. Gold deposits of the NWT: classes, styles, genesis, exploration methods, and success probabilities. In Contributions to the Geology of the Northwest Teritories; edited by J.A. Brophy; D.I.A.N.D., EGS 1984-6, p. 121-129.

Table 1. Stratigraphic Division, Thickness, and a Sampling of Yellowknife Greenstone Belt

Formation		Cycle	Segment	Thickness (m)			Sampling			
	Division						Sample Numbers (#)	No of samples by:		
				Segment	Formation and Division	Belt		Segment	Division	Belt
Banting			F	700	700		43-47	5	5	
Kam	Upper Kam	3	E^2	650	6800	1400	32-35	4	31	47
			E^1	650			29-31	3		
		2	D	2300			b)36-42 a)22-28	7 7		
			C	3200			12-21	10		
	Lower Kam		Townsite flows	600	6500		10,11	2	11	
		1	B	3400			5-9	5		
			A	2500			1-4	4		

Table 2. Number of Samples by Class and Stratigraphic Division

	Lower Kam	Upper Kam	Total Kam	Banting	Yellowknife Belt
Basalt	6	23	29	0	29
Basalt Andesite	3	5	8	0	8
Andesite	0	3	3	1	4
Dacite	2	0	2	4	6
Total	11	31	42	5	47

Table 3. Mean Class Compositions

	Basalt		Basalt-Andesite		Andesite		Dacite	
	Mean	S.D.	Mean	S.D.	Mean	S.D.	Mean	S.D.
N =	29		8		4		6	
wt.%								
SiO_2	50.69	1.43	54.58	1.18	62.52	0.44	65.60	1.95
TiO_2	1.17	0.30	0.80	0.13	0.90	0.16	0.60	0.13
Al_2O_3	13.10	1.09	13.32	2.52	14.90	3.82	16.96	1.41
FeO	13.08	2.72	10.86	1.40	7.23	1.96	4.42	0.25
MnO	0.22	0.03	0.20	0.06	0.13	0.04	0.06	0.01
MgO	7.56	1.65	7.20	1.65	4.68	2.07	1.80	0.37
CaO	10.69	1.96	9.92	1.69	4.33	0.92	3.98	0.76
Na_2O	2.16	0.89	1.94	1.17	3.32	0.81	3.27	0.19
K_2O	0.49	0.37	1.11	1.21	1.67	2.01	3.09	0.30
FeO/MgO	1.60		1.51		1.54		2.46	
FeO/ FeO+MgO	0.63		0.60		0.61		0.71	
ppm								
La	6.8	4.1	7.8	7.5	27.4	13.5	42.4	8.7
Ce	17.1	10.6	12.7	7.3	48.5	8.9	76.3	13.6
Nd	6.8	3.6	7.2	5.2	20.4	8.0	23.3	8.8
Sm	2.7	1.1	2.2	1.1	4.3	1.0	5.7	1.1
Eu	0.9	0.4	0.6	0.2	1.1	0.2	1.2	0.2
Eu_N	12.4		8.3		15.2		16.6	
Eu_N	12.9	5.5	9.5	3.8	16.7	2.1	20.5	3.9
Tb	0.6	0.2	0.4	0.2	0.8	0.3	1.0	0.4
Ho	1.0	0.7	0.7	0.5	1.3	0.5	1.2	0.4
Yb	2.3	0.6	1.8	0.4	1.4	0.9	1.4	1.0
Lu	0.4	0.1	0.3	0.1	0.3	0.1	0.2	0.1

cont'd...

Table 3. Mean Class Compositions

	Basalt		Basalt-Andesite		Andesite		Dacite	
	Mean	S.D.	Mean	S.D.	Mean	S.D.	Mean	S.D.
REE[1]	38.6		33.7		105.5		152.7	
LREE[2]	33.4		29.9		100.6		147.7	
HREE[3]	4.3		3.2		3.8		3.8	
$[La/Yb]_N$	2.0	1.0	3.1	3.1	7.6	0.6	30	15
$[La/Sm]_N$	1.6	0.4	1.9	0.9	3.7	0.9	4.5	0.6
$[Sm/Yb]_N$	1.3	0.4	1.4	0.8	2.3	0.1	6.3	2.9
$[Yb]_N$	10.9	3.0	8.6	1.7	6.5	4.5	6.5	4.8
Eu/Eu*	1.0		0.9		0.9		0.8	
Th	1.4	1.2	1.4	1.0	7.1	2.1	13.6	2.7
Hf	2.2	1.0	1.6	0.6	4.3	0.9	4.6	0.6
Ta	0.2	0.2	0.2	0.1	0.5	0.2	0.7	0.1
Ba	124	91	221	208	494	521	756	206
Sc	37.9	9.4	36.2	7.6	16.8	-	8.8	1.8
Co	53	18	47	19	30	9	15	6
Cr	202	129	392	516	133	56	21	11
Ni	94	32	113	89	66	31	16	10
V	258	39	203	36	134	20	69	11
Zr	82	25	82	51	169	27	189	77
Y	25	6	20	4	23	8	24	16
Sr	111	42	140	113	175	58	223	63
Rb	12	11	29	35	29	44	78	17
Zr/Y	3.3	0.6	3.9	1.6	8.1	2.7	9.1	2.2
Rb/Sr	0.11		0.21		0.17		0.35	
Zr/Hf	37		51		39		41	

Footnotes:

[1]In Tables 3-5 = sum of all nine REE listed in the Table

[2]In Tables 3-5 = sum of La + Ce + Nd + Sm

[3]In Tables 3-5 = sum of Tb + Ho + Yb + Lu

In Tables 3-5, N = number of samples

Table 4 Mean Compositions by Stratigraphic Division

	Kam Formation												
	Lower Kam				Upper Kam								
	Cycle 1				Cycle 2			Cycle 3					
Segment	A	B	Townsite	Complete	C	D+E[1]	Complete	Complete E[2]	Complete	Complete	Banting FM. Complete	Upper Kam + Banting	Yellowknife Complete
Column	1	2	3	4	5	6	7	8	9	10	11	12	13
N[2]	4	5	2	11	10	17	27	4	31	42	5	36	47
wt % SiO_2	51.47	52.54	68.09	53.66	51.40	50.03	50.54	51.51	50.67	52.17	64.02	52.46	53.02
TiO_2	1.37	1.10	0.76	1.17	1.02	0.97	0.99	1.38	1.04	1.08	0.55	0.97	1.04
Al_2O_3	11.12	13.51	15.17	12.76	13.28	13.20	13.23	14.10	13.34	13.05	18.36	14.02	13.43
FeO	14.31	12.76	4.42	12.55	12.40	11.86	12.06	13.65	12.27	12.41	4.36	11.20	11.84
MnO	0.27	0.24	0.06	0.23	0.21	0.20	0.20	0.19	0.20	0.22	0.06	0.18	0.21
MgO	6.09	6.50	1.44	5.83	7.10	8.50	7.98	6.34	7.77	6.80	1.92	6.98	6.45
CaO	12.54	10.69	3.20	10.68	10.96	9.10	9.79	8.91	9.68	10.18	4.09	8.92	9.75
Na_2O	1.94	2.25	3.31	2.23	2.79	2.12	2.37	2.06	2.33	2.28	3.06	2.43	2.34
K_2O	0.39	0.54	3.13	0.74	0.42	0.68	0.58	1.31	0.67	0.71	3.39	0.68	0.90
P_2O_5	0.20	0.12	0.29	0.17	0.08	0.12	0.11	0.21	0.12	0.15	0.14	0.12	0.14
Fe/MgO	2.35	1.96	3.07	2.23	1.75	1.40	1.51	2.15	1.59	1.91	2.27	1.68	1.94
FeO/FeO + MgO	0.70	0.66	0.76	0.69	0.64	0.59	0.60	0.68	0.61	0.65	0.70	0.62	0.65
ppm													
La	6.2	5.5	41.6	9.4	5.5	8.5	7.3	17.9	8.7	9.1	43.6	13.4	11.6
Ce	17.9	13.0	63.4	20.0	13.3	18.7	16.7	28.4	18.2	19.1	78.5	26.4	23.3
Nd	8.0	6.2	30.2	9.3	6.0	7.6	7.0	12.2	7.7	8.5	22.3	9.7	9.5
Sm	3.1	2.3	6.5	3.0	2.1	2.6	2.4	4.6	2.7	2.8	5.4	3.1	3.0
Eu	1.1	0.8	1.1	1.0	0.7	0.8	0.8	1.2	0.8	0.9	1.2	0.9	0.9

cont'd... Table 4 Mean Compositions by Stratigraphic Division

	Kam Formation												
	Lower Kam				Upper Kam								
	Cycle 1				Cycle 2			Cycle 3					
Segment	A	B	Townsite	Complete	C	D+E[1]	Complete	Complete E[2]	Complete	Complete	Banting FM Complete	Upper Kam + Banting	Yellowknife Complete
Column	1	2	3	4	5	6	7	8	9	10	11	12	13
N[2]	4	5	2	11	10	17	27	4	31	42	5	36	47
Eu_N	15.1	10.5	15.0	12.8	9.3	11.6	10.7	16.7	11.5	12.2	15.9	12.1	12.5
Eu^*_N	16.9	11.4	24.2	14.9	9.6	12.2	11.2	19.0	12.2	13.6	18.0	13.0	13.9
Tb	0.8	0.6	0.5	0.7	0.5	0.6	0.5	0.7	0.5	0.6	1.2	0.6	0.6
Ho	1.7	0.9	1.2	1.3	0.6	1.0	0.9	0.8	0.9	1.1	1.4	1.0	1.1
Yb	2.6	2.3	2.6	2.5	2.1	2.0	2.0	2.5	2.1	2.3	0.6	2.1	2.2
Lu	0.4	0.4	0.3	0.4	0.3	0.3	0.3	0.4	0.3	0.3	0.2	0.3	0.3
REE	41.8	32.0	147.4	56.4	31.1	42.1	37.9	68.7	41.9	44.7	154.4	57.5	52.5
LREE	35.2	27.0	141.7	50.8	26.9	37.4	33.4	63.1	37.3	39.5	149.8	52.6	47.4
HREE	5.5	4.2	4.6	4.6	3.5	3.9	3.7	4.4	3.8	4.3	3.4	4.0	4.2
$[La/Yb]_N$	1.8	1.6	10.0	2.5	1.9	3.0	2.6	5.4	3.0	2.8	39.4	7.9	5.
$[La/Sm]_N$	1.4	1.4	3.9	1.7	1.5	1.9	1.8	2.3	1.9	1.8	4.9	2.3	2.0
$[Sm/Yb]_N$	1.3	1.0	2.7	1.3	1.1	1.5	1.4	2.1	1.5	1.4	8.1	2.4	1.9
Eu/Eu*	0.9	1.0	0.6	0.9	1.0	1.0	1.02	0.9	1.0	1.0	0.9	1.0	1.0
$[Yb]_N$	12.5	11.0	12.7	11.8	10.1	9.4	9.6	11.2	9.8	10.8	2.8	8.9	10.2
Th	1.4	1.1	11.1	2.2	1.2	2.3	1.9	2.1	1.9	2.1	13.9	3.5	2.9
Hf	2.7	1.9	4.7	2.5	1.7	2.3	2.1	2.7	2.2	2.4	4.5	2.5	2.6
Ta	0.3	0.2	0.8	0.3	0.2	0.3	0.2	0.3	0.2	0.3	0.6	0.3	0.3
Ba	95	185	624	193	100	110	106	300	131	162	910	236	215

cont'd... Table 4 Mean Compositions by Stratigraphic Division

	Kam Formation												
	Lower Kam				Upper Kam								
	Cycle 1				Cycle 2			Cycle 3					
Segment	A	B	Townsite	Complete	C	D+E[1]	Complete	Complete E[2]	Complete	Complete	Banting FM Complete	Upper Kam + Banting	Yellowknife Complete
Column	1	2	3	4	5	6	7	8	9	10	11	12	13
N[2]	4	5	2	11	10	17	27	4	31	42	5	36	47
Sc	44.3	36.0	7.6	36.5	38.0	33.4	35.1	33.9	34.9	35.7	10.0	31.5	33.9
Co	67	46	12	51	44	49	48	56	49	50	20	45	48
Cr	526	285	5	353	186	219	206	88	191	272	34	170	255
Ni	171	133	9	136	102	109	106	96	105	121	29	95	114
V	298	295	47	271	262	250	254	211	248	260	93	227	248
Zr	92	84	320	111	71	91	84	143	93	102	148	100	105
Y	26	24	40	26	21	20	21	24	21	24	12	20	23
Sr	95	190	147	148	134	102	114	131	116	132	253	135	141
Rb	14	12	96	21	8	15	13	33	16	19	69	23	23
Zr/Y	3.5	3.5	8.0	4.3	3.4	4.6	4.0	5.9	4.4	4.3	12.3	5.0	4.6
Rb/Sr	0.15	0.06	0.65	0.14	0.06	0.15	0.11	0.25	0.14	0.14	0.27	0.17	0.16
Zr/Hf	34	44	68	44	42	40	40	53	42	43	33	40	40

[1]Weighted by number of samples within segments and by stratigraphic thicknesses (Table 1) between divisions.

[2]N = number of samples.

Table 5. Mean Class Compositions by Segment, Cycle and Formation

	Kam Formation											Banting Formation	
	Cycle 1				Cycle 2					Cycle 3			
Segment	Basalt		Basalt Andesite	Dacite	Basalt			Basalt Andesite	Andesite	Basalt	Basalt Andesite	Andesite	Dacite
	A	B			C	D	DH 919						
Column	1	2	3	4	5	6	7	8	9	10	11	12	13
N	3	3	3	2	8	6	6	4	3	3	1	1	4
wt %													
SiO_2	49.98	51.57	54.63	68.09	50.80	51.17	50.36	54.03	62.47	49.80	56.62	62.66	64.36
TiO_2	1.61	1.35	0.70	0.76	1.06	1.01	0.98	0.76	0.97	1.50	1.01	0.67	0.52
Al_2O_3	11.70	13.77	11.87	15.17	13.32	12.78	13.52	13.41	13.08	13.02	17.35	20.38	17.86
FeO	14.98	13.70	11.67	4.42	12.68	12.50	13.32	11.13	8.20	15.60	7.81	4.33	4.39
MnO	0.26	0.27	0.24	0.06	0.21	0.21	0.22	0.20	0.14	0.22	0.11	0.07	0.06
MgO	5.49	5.85	7.59	1.44	7.10	8.33	10.13	7.75	5.67	7.18	3.82	1.71	1.98
CaO	12.75	10.13	11.66	3.20	11.31	10.81	9.79	9.02	4.76	9.11	8.32	3.01	4.37
Na_2O	2.41	2.32	1.62	3.31	2.65	2.25	1.22	2.53	3.66	2.55	0.58	2.29	3.25
K_2O	0.26	0.47	0.69	3.13	0.38	0.51	0.78	0.72	0.67	0.42	3.96	4.65	3.07
P_2O_5	0.16	0.16	0.06	0.29	0.08	0.08	0.16	0.07	0.15	0.21	0.20	0.10	0.16
FeO/MgO	2.72	2.34	1.54	3.20	1.79	1.50	1.37	1.46	1.45	2.17	2.04	2.53	2.24
FeO/FeO+MgO	0.73	0.70	0.61	0.76	0.64	0.60	0.57	0.59	0.59	0.69	0.67	0.72	0.72
ppm													
La	6.7	6.5	4.3	41.7	5.4	5.3	6.1	6.0	20.9	15.6	25.1	46.8	42.8
Ce	19.5	16.8	9.1	63.4	12.6	9.5	14.3	15.3	44.2	33.7	12.6	61.3	82.8
Nd	9.1	7.5	4.5	30.2	6.2	3.9	7.1	6.3	16.5	10.0	18.7	37.2	19.9
Sm	3.7	2.6	1.7	6.5	2.1	2.2	2.5	1.9	3.9	4.5	4.9	5.6	5.3

cont'd... Table 5. Mean Class Compositions by Segment, Cycle and Formation

	Kam Formation											Banting Formation	
	Cycle 1				Cycle 2					Cycle 3			
	Basalt		Basalt Andesite	Dacite	Basalt			Basalt Andesite	Andesite	Basalt	Basalt Andesite	Andesite	Dacite
Segment	A	B			C	D	DH 919						
Column	1	2	3	4	5	6	7	8	9	10	11	12	13
N	3	3	3	2	8	6	6	4	3	3	1	1	4
Eu	1.3	0.8	0.6	1.1	0.7	0.7	0.9	0.6	1.1	1.4	0.7	0.8	1.2
Eu_N	17.4	11.5	8.7	15.0	9.6	9.0	12.4	8.8	15.7	19.2	9.3	11.8	17.0
Eu^*_N	19.3	13.7	8.4	24.2	10.4	10.2	12.3	8.3	17.2	19.5	17.5	15.3	18.7
Tb	0.9	0.7	0.4	0.5	0.5	0.5	0.5	0.5	0.7	0.8	0.3	0.9	1.3
Ho	2.0	0.8	0.9	1.2	0.5	0.5	1.6	0.8	1.1	1.0	0	2.0	1.3
Yb	3.0	2.4	2.0	2.6	2.2	2.0	2.1	1.7	1.8	2.8	1.7	0	0.7
Lu	0.5	0.3	0.3	0.3	0.4	0.3	0.3	0.3	0.3	0.4	0.3	0.5	0.1
REE	46.7	38.4	23.8	147.5	30.6	24.9	35.4	33.4	90.5	70.2	64.3	155.2	155.4
LREE	39.0	33.4	19.6	141.8	26.3	20.9	30.0	29.5	85.5	63.8	61.3	150.9	150.8
HREE	6.4	4.2	3.6	4.6	3.6	3.3	4.5	3.3	3.9	5.0	2.3	3.4	3.4
$[La/Yb]_N$	1.7	1.8	1.5	10.5	1.8	1.9	2.0	2.7	7.6	3.8	10.0	-	39.4
$[La/Sm]_N$	1.2	1.5	1.6	3.9	1.5	1.6	1.6	1.8	3.2	2.0	3.2	5.1	4.9
$[Sm/Yb]_N$	1.4	1.1	1.0	2.7	1.1	1.3	1.4	1.3	2.3	1.8	3.2	-	8.1
Eu/Eu*	1.0	0.8	1.1	0.6	1.08	1.04	1.1	1.1	0.9	1.0	0.5	0.8	0.9
$[Yb]_N$	14.2	11.3	9.5	12.7	10.4	9.7	9.9	8.1	8.7	13.3	4.9	-	2.8
Th	1.5	1.2	1.0	11.1	1.1	1.6	1.2	1.8	6.2	2.4	1.2	9.9	14.9
Hf	3.0	2.3	1.4	4.7	1.8	1.9	2.0	1.7	4.3	3.1	1.4	4.3	4.6
Ta	0.4	0.2	0.2	0.8	0.2	0.2	0.3	0.2	0.5	0.4	0.2	0.5	0.6
Ba	73	184	178	624	101	71	181	136	236	169	691	1263	822

cont'd... Table 5. Mean Class Compositions by Segment, Cycle and Formation

	Kam Formation											Banting Formation	
	Cycle 1				Cycle 2					Cycle 3			
	Basalt		Basalt Andesite	Dacite	Basalt			Basalt Andesite	Andesite	Basalt	Basalt Andesite	Andesite	Dacite
Segment	A	B			C	D	DH 919						
Column	1	2	3	4	5	6	7	8	9	10	11	12	13
N	3	3	3	2	8	6	6	4	3	3	1	1	4
Sc	44.3	37.0	37.7	7.6	40.3	30.8	41.8	34.7	17.4	32.6	37.5	12.0	9.5
Co	62	46	59	12	46	46	64	39	28	62	38	37	16
Cr	92	257	827	5	185	247	210	238	135	104	37	71	25
Ni	84	145	220	9	98	114	109	113	96	117	34	54	23
V	327	332	231	47	266	268	279	249	165	241	122	126	85
Zr	106	98	57	320	72	69	76	67	183	117	203	145	149
Y	29	28	17	40	22	21	20	17	24	24	25	11	12
Sr	96	129	218	147	131	114	78	103	151	148	79	213	263
Rb	3	13	21	96	9	11	18	14	13	8	106	90	64
Zr/y	3.7	3.5	3.2	8.0	3.4	3.4	3.5	3.8	7.7	4.8	9.0	13.0	12.4
Rb/Sr	0.03	0.10	0.10	0.65	0.07	0.10	0.23	0.14	0.09	0.05	1.34	0.42	0.24
Zr/Hf	35	43	41	68	40	36	38	39	43	38	145	34	12

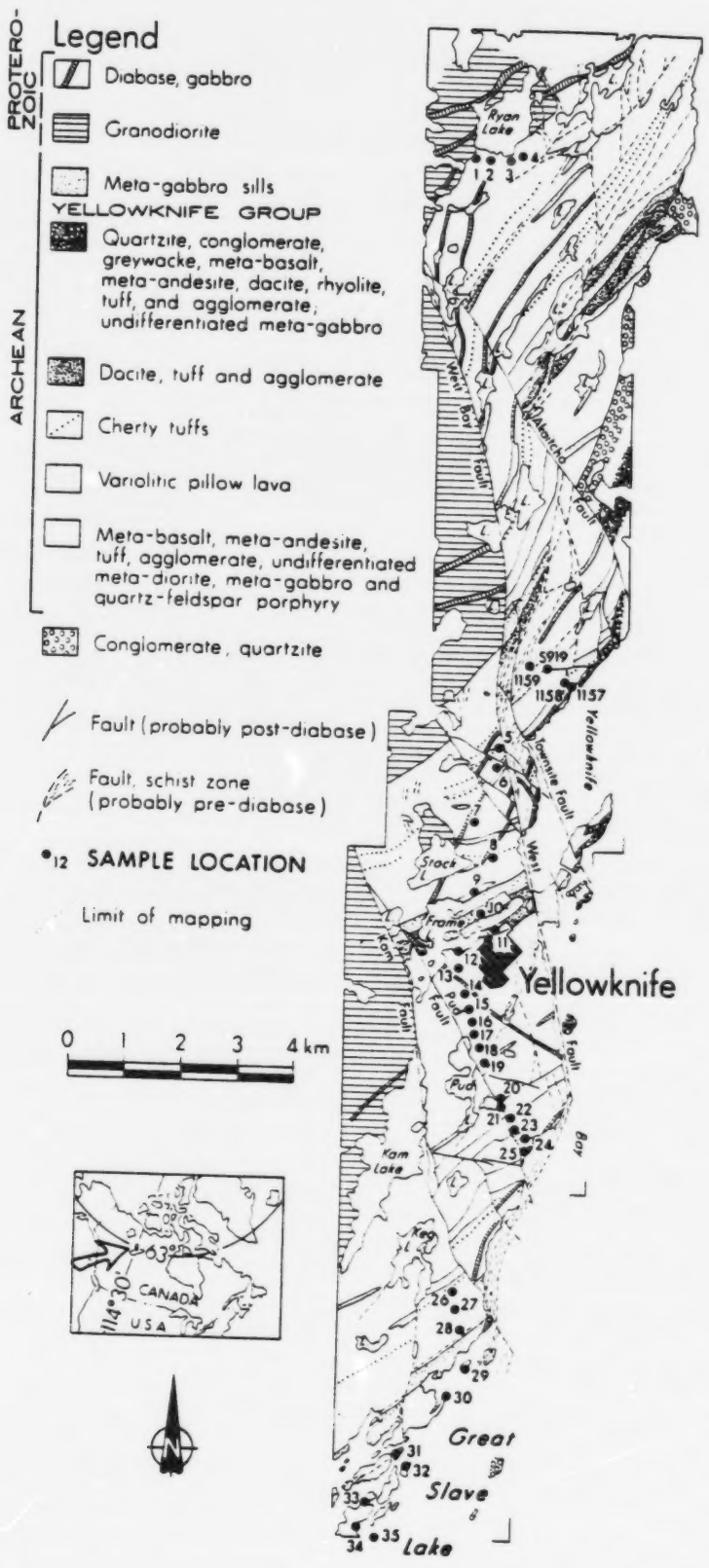
Legend
PROTERO-ZOIC
Diabase, gabbro
Granodiorite
ARCHEAN
Meta-gabbro sills
YELLOWKNIFE GROUP
Quartzite, conglomerate, greywacke, meta-basalt, meta-andesite, dacite, rhyolite, tuff, and agglomerate; undifferentiated meta-gabbro
Dacite, tuff and agglomerate
Cherty tuffs
Variolitic pillow lava
Meta-basalt, meta-andesite, tuff, agglomerate, undifferentiated meta-diorite, meta-gabbro and quartz-feldspar porphyry
Conglomerate, quartzite
Fault (probably post-diabase)
Fault, schist zone (probably pre-diabase)
12 SAMPLE LOCATION
Limit of mapping
0 1 2 3 4 km
CANADA
USA
Yellowknife
Ryan Lake
Great Slave Lake
Kam Lake
Frame
Stock
Pud
Yellowknife Fault
Townsite Fault
Kam Fault
Pud Fault
Fault
Bay

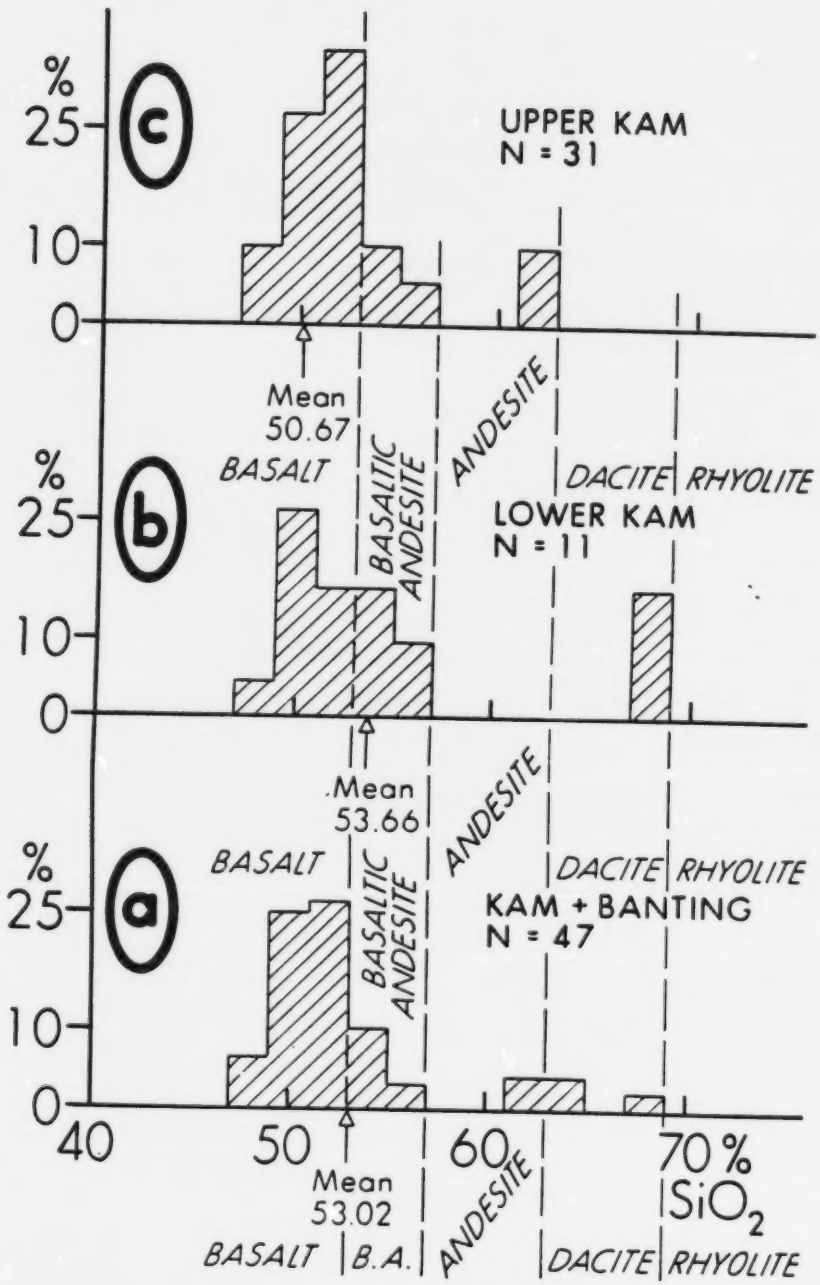
%
25
10
0
c
UPPER KAM
N = 31
Mean
50.67
BASALT
BASALTIC ANDESITE
ANDESITE
DACITE
RHYOLITE
b
LOWER KAM
N = 11
Mean
53.66
a
KAM + BANTING
N = 47
Mean
53.02
B.A.
40
50
60
70 %
SiO_2

#2

Fig 3A

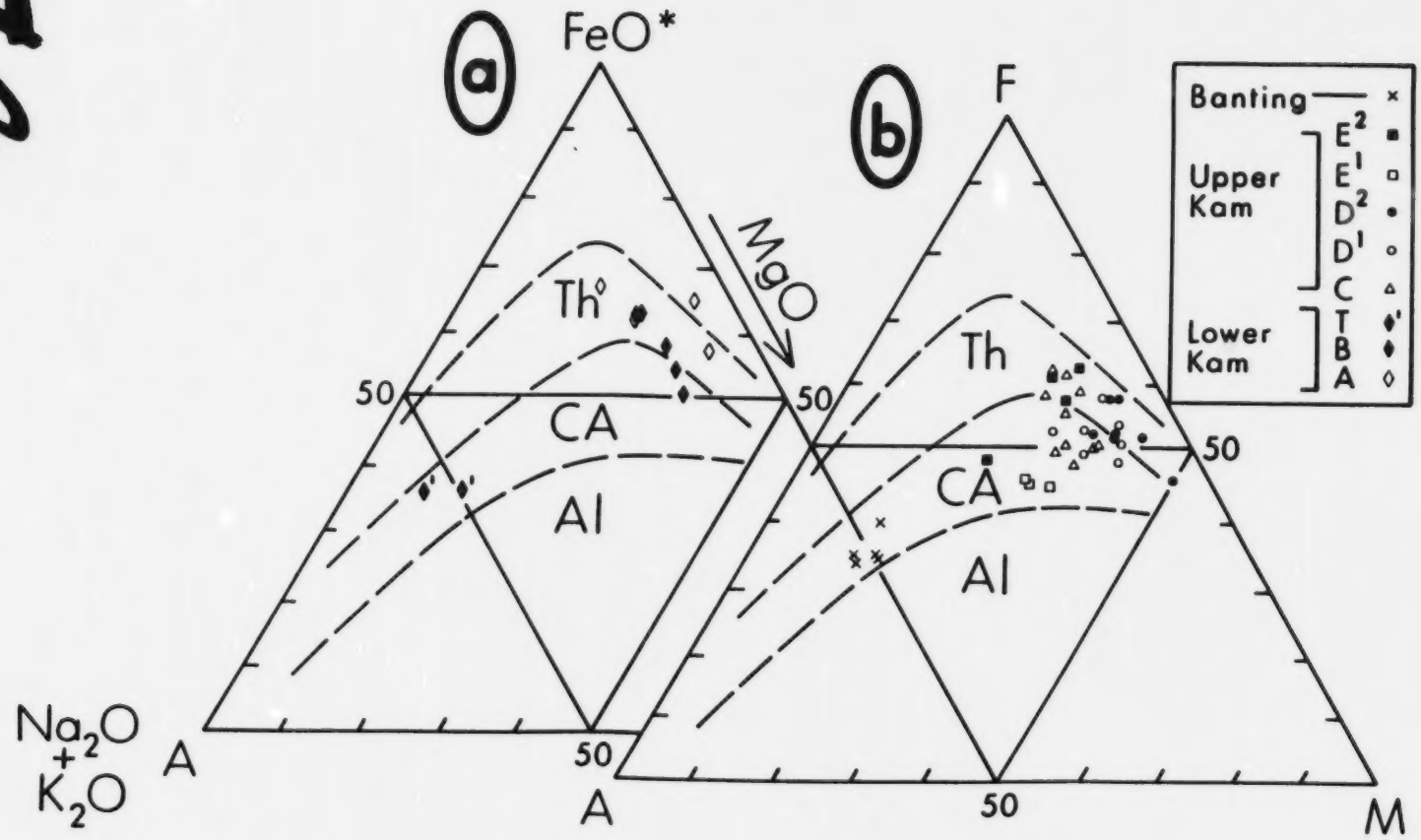
a
FeO*
MgO
Th
CA
Al
50
50
50
Na_2O + K_2O
A
A
b
F
Th
CA
Al
50
50
M
Banting
Upper Kam
E^2
E^1
D^2
D^1
C
Lower Kam
T
B
A

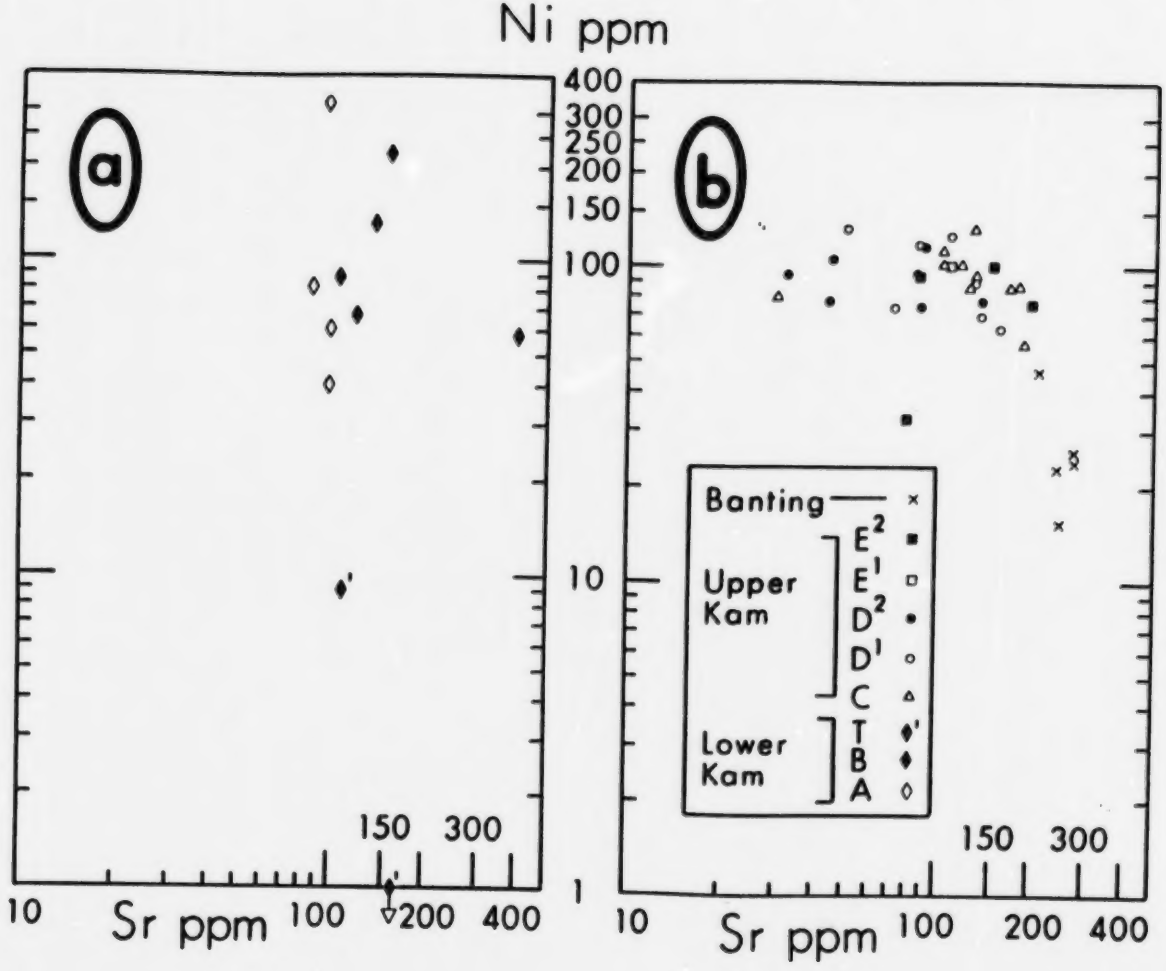
Ni ppm
400
300
250
200
150
100
10
1
a
b
150 300
10
Sr ppm
100
200
400
Banting
Upper Kam
Lower Kam
E2
E1
D2
D1
C
T
B
A

Fig

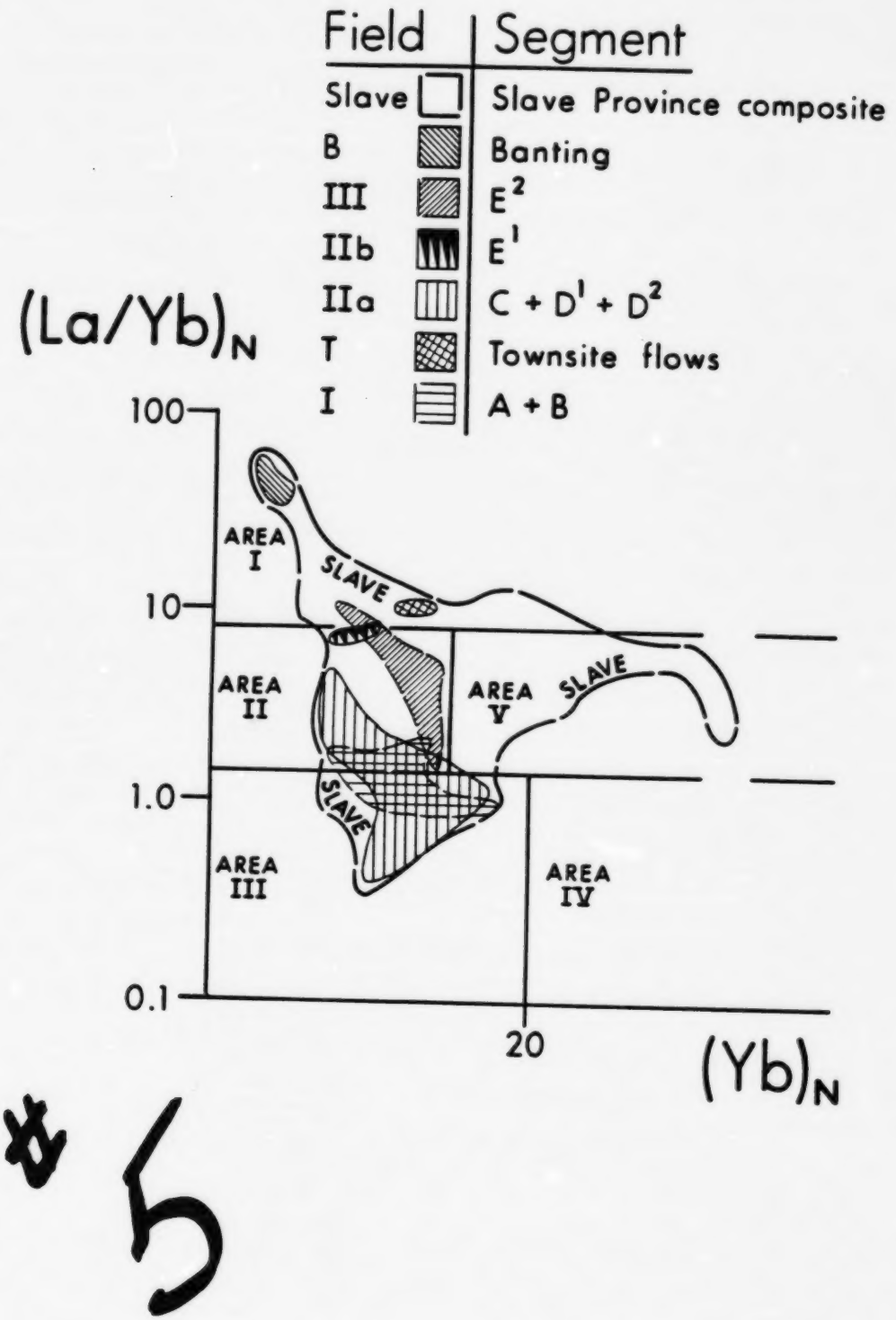
Field
Segment
Slave
Slave Province composite
B
Banting
III
E²
IIb
E¹
IIa
C + D¹ + D²
T
Townsite flows
I
A + B
(La/Yb)N
100
10
1.0
0.1
20
(Yb)N
AREA I
AREA II
AREA III
AREA IV
AREA V
SLAVE
SLAVE
SLAVE

5

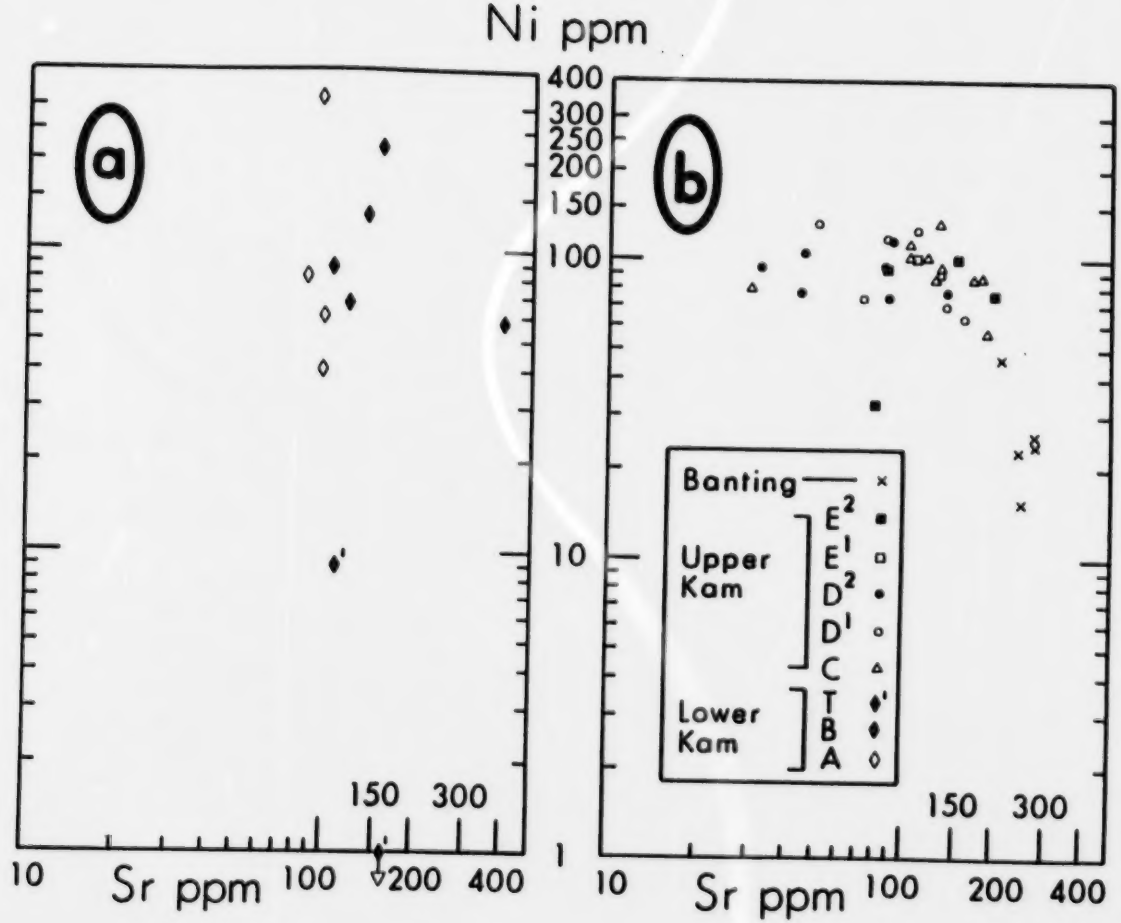
Ni ppm
400
300
250
200
150
100
10
1
a
b
150 300
10
Sr ppm
100
200
400
Banting
Upper Kam
E2
E1
D2
D1
C
Lower Kam
T
B
A

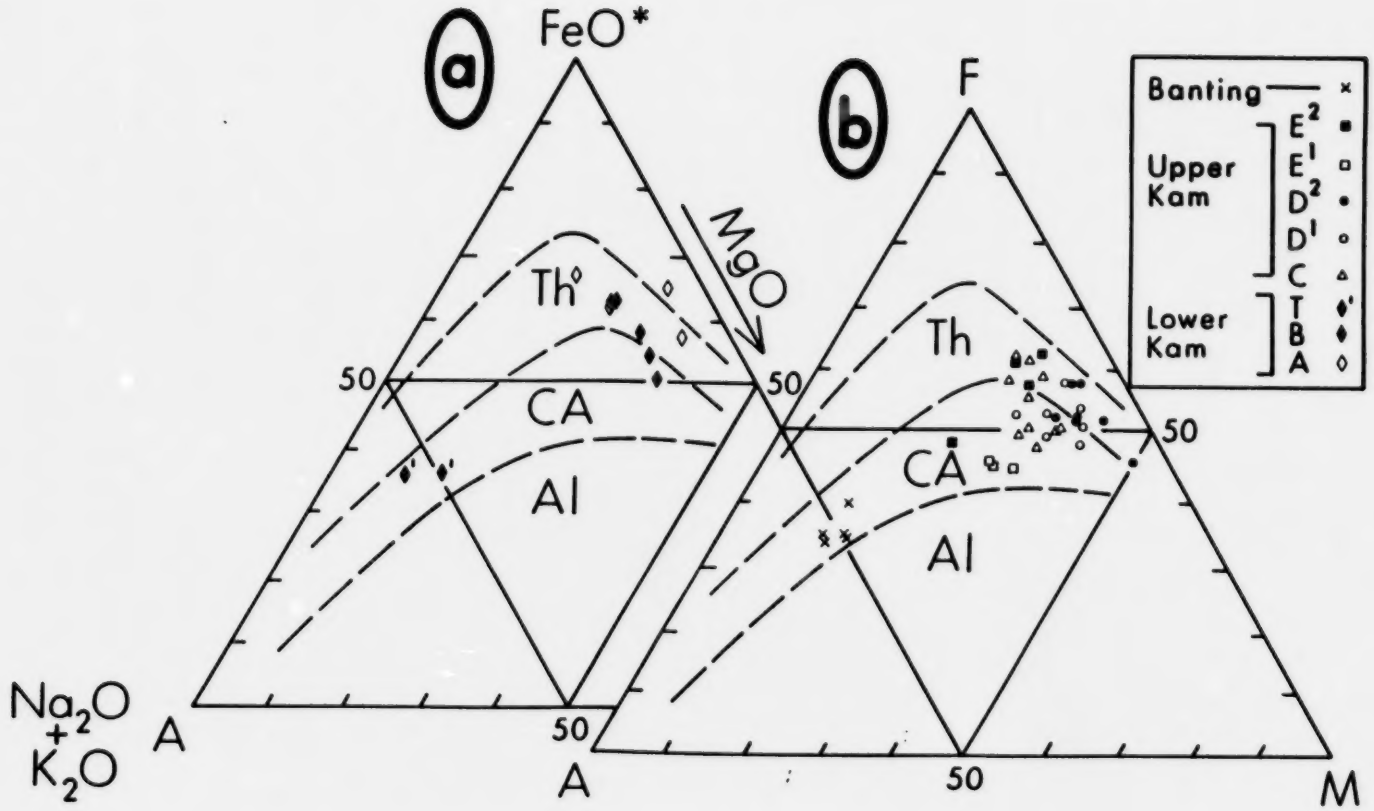
a
FeO*
MgO
Th
CA
Al
50
50
50
Na2O
+
K2O
A
A
b
F
Th
CA
Al
50
50
M
Banting
Upper Kam
E2
E1
D2
D1
C
Lower Kam
T
B
A